

実証炉用36本燃料装荷炉心の冷却材
ボイド反応度の測定(データ集)

1988年10月

動力炉・核燃料開発事業団
大洗工学センター

複製又はこの資料の入手については、下記にお問い合わせください。

〒311-13 茨城県東茨城郡大洗町成田町4002

動力炉・核燃料開発事業団

大洗工学センター システム開発推進部・技術管理室

Enquires about copyright and reproduction should be addressed to: Technology Management Section O-arai Engineering Center, Power Reactor and Nuclear Fuel Development Corporation 4002 Narita-cho, O-arai-machi, Higashi-Ibaraki, Ibaraki-ken, 311-13, Japan

動力炉・核燃料開発事業団 (Power Reactor and Nuclear Fuel Development Corporation)

実証炉用36本燃料装荷炉心の冷却材ボイド反応度の測定

小綿 泰樹* 戸村 和二* 佐々木喜行*

岡崎 庸** 葉山 勇**

要 旨

ATR 実証炉に使われている燃料と同一形状の燃料体を装荷した炉心において、試験燃料体の燃料組成を変化させた場合の冷却材ボイド反応度を把握し、核設計コードの精度評価に寄与する。

実証炉用燃料体を DCA (重水臨界実験装置) 炉心の中央部に部分装荷して冷却材ボイド反応度を臨界水位差法により測定した。試験燃料体は下表に示すように、 UO_2 及び MOX の両組成ごとに集合体各層の濃縮度 (富化度) 分布を変化させ、それぞれ 2 種 (タイプ I, II), 3 種 (タイプ III ~ V) の計 5 種類である。まずタイプ I 燃料体を炉心中央部の (3×3) チャンネルに装荷し、次に炉心中心チャンネルの燃料体 1 体を順次タイプ II, III, IV 又は V の燃料体に置き換えてボイド反応度を測定した。なお、試験燃料以外の燃料 (1.2 wt% UO_2) チャンネルは常に 100% ボイドとした。

ボイド反応度は集合体内に濃縮度 (富化度) 分布がないか、又は小さければ、ボイド率の増加とともに単調に負側に移行する。しかし、集合体内に濃縮度 (富化度) 差を設ければ、局所出力分布の平坦化とは裏腹にボイド反応度は正側へ移行する。

表 36 本試験燃料体の種類

燃料体 タイプ	組 成	^{235}U or Pu^{f1s} 濃縮 (富化) 度 (wt%)			
		() : 公称濃縮 (富化) 度 (wt%)			
		内 層	中間層	外 層	平 均
I	UO_2	2.687 (2.7)	2.687 (2.7)	2.687 (2.7)	2.687 (2.7)
II	UO_2	3.188 (3.2)	3.188 (3.2)	2.188 (2.2)	2.688 (2.7)
III	PuO_2-UO_2	3.345 (3.3)	3.345 (3.3)	3.345 (3.3)	3.345 (3.3)
IV	PuO_2-UO_2	3.345 (3.3)	3.345 (3.3)	1.567 (1.6)	2.456 (2.5)
V	PuO_2-UO_2	3.345 (3.3)	3.345 (3.3)	1.170 (1.2)	2.257 (2.3)

* 大洗工学センター実験炉部 臨界工学試験室

** 現 三菱重工業株式会社

October 1988

Measurement of Coolant Void Reactivity in the Core
Fueled with 36-rod Clusters

Yasuki Kowata^{*}, Kazuji Tomura^{*}
Yoshiyuki Sasaki^{*}, Isao Okazaki^{**}
and Isamu Hayama^{**}

Abstract

Behavior of coolant void reactivity due to change in fissile enrichment or composition of 36-rod test fuel cluster has been clarified in the core fueled with the same form fuel assembly as that of Fugen type demonstration reactor. Experimental results will contribute to the investigation of design code WIMS concerning accuracy for the test fuel lattice.

The test fuel clusters were loaded in the central (3×3) channels and/or in those one channel. The test clusters consist of five types in all as shown in the following table ; two types of UO₂ and three types of PuO₂-UO₂. Void reactivities were measured by means of the critical level difference method. In the measurement of void reactivities, nine type I clusters were loaded in the (3×3) channels of the core, and the test cluster of the center channel was replaced with type II, III, IV or V test cluster. Driver fuel (28-rod 1.2 wt% UO₂) channels were made always to be as an air coolant (100%-voided) condition.

The void reactivity shifted farther to the negative side as the void fraction increased, if there was no or small distribution of enrichment in the cluster. However, the void reactivity shifted to the positive side compared with the case of no distribution, if the distribution of enrichment was provided in the cluster.

* O-arai Engineering Center, Experimental Reactor Division,
Critical Engineering Section

** Mitsubishi Heavy Industry Co., Ltd.

Table Types of 36-rod Test Fuel Cluster

Types of Cluster	Composition	^{235}U or Pu^{fiss} Enrichment (wt%) () : Nominal Enrichment (wt%)			
		Inner	Middle	Outer	Average
I	UO_2	2.687 (2.7)	2.687 (2.7)	2.687 (2.7)	2.687 (2.7)
II	UO_2	3.188 (3.2)	3.188 (3.2)	2.188 (2.2)	2.688 (2.7)
III	$\text{PuO}_2\text{-UO}_2$	3.345 (3.3)	3.345 (3.3)	3.345 (3.3)	3.345 (3.3)
IV	$\text{PuO}_2\text{-UO}_2$	3.345 (3.3)	3.345 (3.3)	1.567 (1.6)	2.456 (2.5)
V	$\text{PuO}_2\text{-UO}_2$	3.345 (3.3)	3.345 (3.3)	1.170 (1.2)	2.257 (2.3)

目 次

1. 実験条件	1
2. 冷却材ボイド反応度の測定	9
3. 軸方向反射体節約の測定	20

1. Experimental Conditions

Table 1.1 Types of 36-rod Test Fuel Cluster Used in the Center Channel or Central 9 Channels

Table 1.2 Ingredients of Plutonium or Uranium in $\text{PuO}_2\text{-UO}_2$ Pellet

Table 1.3 Ingredients in Test Fuel Pellets

Table 1.4 Specification of Fuel Pellet

Table 1.5 Specification of Composed Material of the Core

Table 1.6 Specification of Coolant and Moderator

Table 1.7 Analysis Results of Poison Concentration in D_2O Moderator

Fig. 1.1 Configuration of DCA core fueled with 36-rod test clusters in central channels.

Fig. 1.2 Cross-sectional view of type I~V 36-rod test cluster

Fig. 1.3 Cross-sectional view of 28-rod UO_2 cluster used in the driver region.

Table 1.1 Types of 36-rod Test Fuel Cluster Used in the Center Channel or Its Surrounding 8 Channels

Types of Cluster	Composition	^{235}U or Pu^{fis} Enrichment (wt%)			
		() : Nominal Enrichment (wt%)			
		Inner	Middle	Outer	Average
I	UO_2	2.687 (2.7)	2.687 (2.7)	2.687 (2.7)	2.687 (2.7)
II	UO_2	3.188 (3.2)	3.188 (3.2)	2.188 (2.2)	2.688 (2.7)
III	$\text{PuO}_2\text{-UO}_2$	3.345 (3.3)	3.345 (3.3)	3.345 (3.3)	3.345 (3.3)
IV	$\text{PuO}_2\text{-UO}_2$	3.345 (3.3)	3.345 (3.3)	1.567 (1.6)	2.456 (2.5)
V	$\text{PuO}_2\text{-UO}_2$	3.345 (3.3)	3.345 (3.3)	1.170 (1.2)	2.257 (2.3)

Table 1.2 Ingredients of Plutonium or Uranium in $\text{PuO}_2\text{-UO}_2$ Pellet

Isotope of Plutonium	Ingredient (wt%)	Isotope of Plutonium	Ingredient (wt%)
^{238}Pu	0.38	^{234}U	0.01
^{239}Pu	67.25	^{235}U	0.73
^{240}Pu	21.75	^{236}U	0.02
^{241}Pu	7.27	^{238}U	99.24
^{242}Pu	2.90		
^{241}Am	1.42		

Table 1.3 Ingredients in Test Fuel Pellets

Nuclide	Ingredient (wt%)					
	2.7wt%UO ₂	3.2wt%UO ₂	2.2wt%UO ₂	3.3wt%MOX	1.6wt%MOX	1.2wt%MOX
U-234	-	-	-	0.009	0.009	0.009
U-235	2.367	2.809	1.928	0.615	0.630	0.633
U-236	-	-	-	0.017	0.017	0.017
U-238	85.733	85.291	86.172	83.545	85.663	86.038
Pu-238	-	-	-	0.032	0.015	0.011
Pu-239	-	-	-	2.662	1.247	0.930
Pu-240	-	-	-	0.861	0.404	0.301
Pu-241	-	-	-	0.242	0.113	0.085
Pu-242	-	-	-	0.115	0.054	0.040
Am-241	-	-	-	0.102	0.048	0.036
O-16	11.900	11.900	11.900	11.800	11.800	11.900

Table 1.4 Specification of Fuel Pellet

Composition	Cluster Type Included	Diameter (mm)	Density (g/cm ³)	Content Ratio of Metal (wt%)
2.7wt% UO ₂	I	12.40	10.332	88.1
3.2wt% UO ₂	II	12.39	10.344	88.1
2.2wt% UO ₂	II	12.40	10.352	88.1
3.3wt%PuO ₂ -UO ₂	III, IV, V	12.43	10.326	88.2
1.6wt%PuO ₂ -UO ₂	IV	12.43	10.302	88.2
1.2wt%PuO ₂ -UO ₂	V	12.46	10.226	88.1

Table 1.5 Specification of Composed Material of the Core

Item		Outer Diameter (.mm)	Thickness (mm)	Density (g/cm ³)	Material
Sheath	Test Fuel(Center)	14.50	0.90	6.523	Zircaloy-2
	Test Fuel(8 Ch)	14.50	0.90	6.523	Zircaloy-2
	Driver Fuel	16.73	0.85	2.67	Alminum
Pressure Tube		120.8	2.0	2.67	Alminum
Calandria Tube		136.5	2.0	2.67	Alminum

Table 1.6 Specification of Coolant and Moderator

(1) Coolant

Simulated Void Fraction (%)	Content (wt%)				Density (g/cm ³)
	H ₂ O	D ₂ O	H ₃ BO ₃	Air	
0	100.00	-	-	-	0.9978
30	63.17	36.82	0.0092	-	1.0348
70	18.07	81.91	0.0215	-	1.0840
100	-	-	-	100.00	0.0012

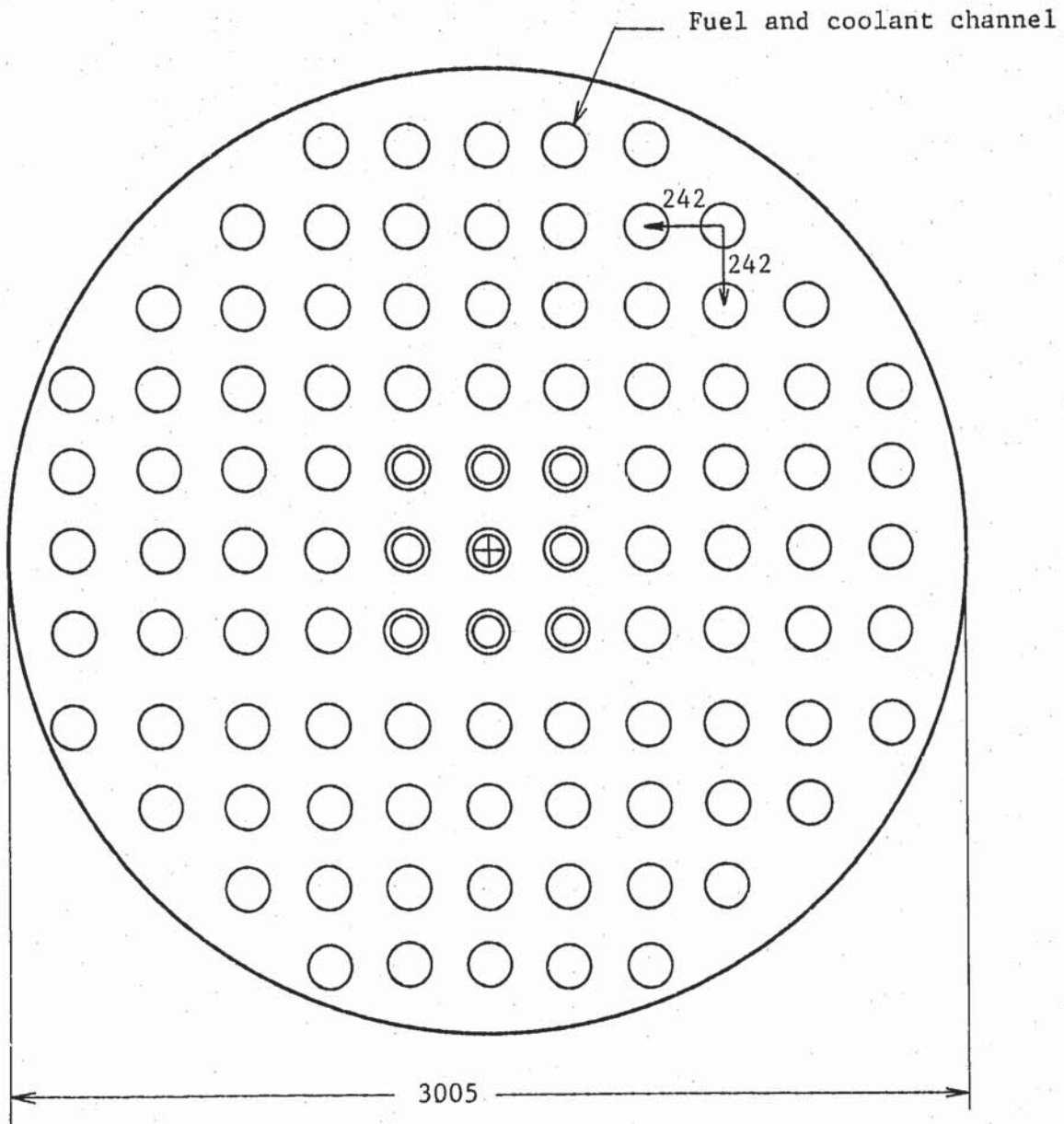
(2) Moderator

D ₂ O Purity	99.1 mol%
Density	1.1040 g/cm ³
¹⁰ B Content	9.869 ppm

Table 1.7 Analysis Results of Poison Concentration in D₂O Moderator and Simulated Coolants

Content		D ₂ O Moderator	Simulated Void Coolant	
			30%	70%
¹⁰ B	(ppm,wt)	9.869 ± 0.014	2.922 ± 0.003	4.869 ± 0.009
Total B (ppm,wt)		34.83 ± 0.04	15.90 ± 0.02	26.50 ± 0.03
¹¹ B/ ¹⁰ B	Atomic No.	2.300 ± 0.001	4.042 ± 0.002	4.041 ± 0.003
	Atomic Wt.*	2.529 ± 0.002	4.444 ± 0.003	4.443 ± 0.003

* Atomic Weight : ¹¹B = 11.009, ¹⁰B = 10.013



Total number of fuel channels : 97

- ⊕ 36 rod UO_2 or PuO_2-UO_2 cluster
(Type I,II,III,IV or V :
0, 30, 70 or 100% void)
- ⊙ 36 rod 2.7 wt% UO_2 cluster
(Type I : 0, 30, 70 or 100% void)
- 28 rod 1.2 wt% UO_2 cluster
(88 channels : 100% void)

Fig. 1.1 Configuration of DCA core fueled with 36-rod test clusters in central channels.

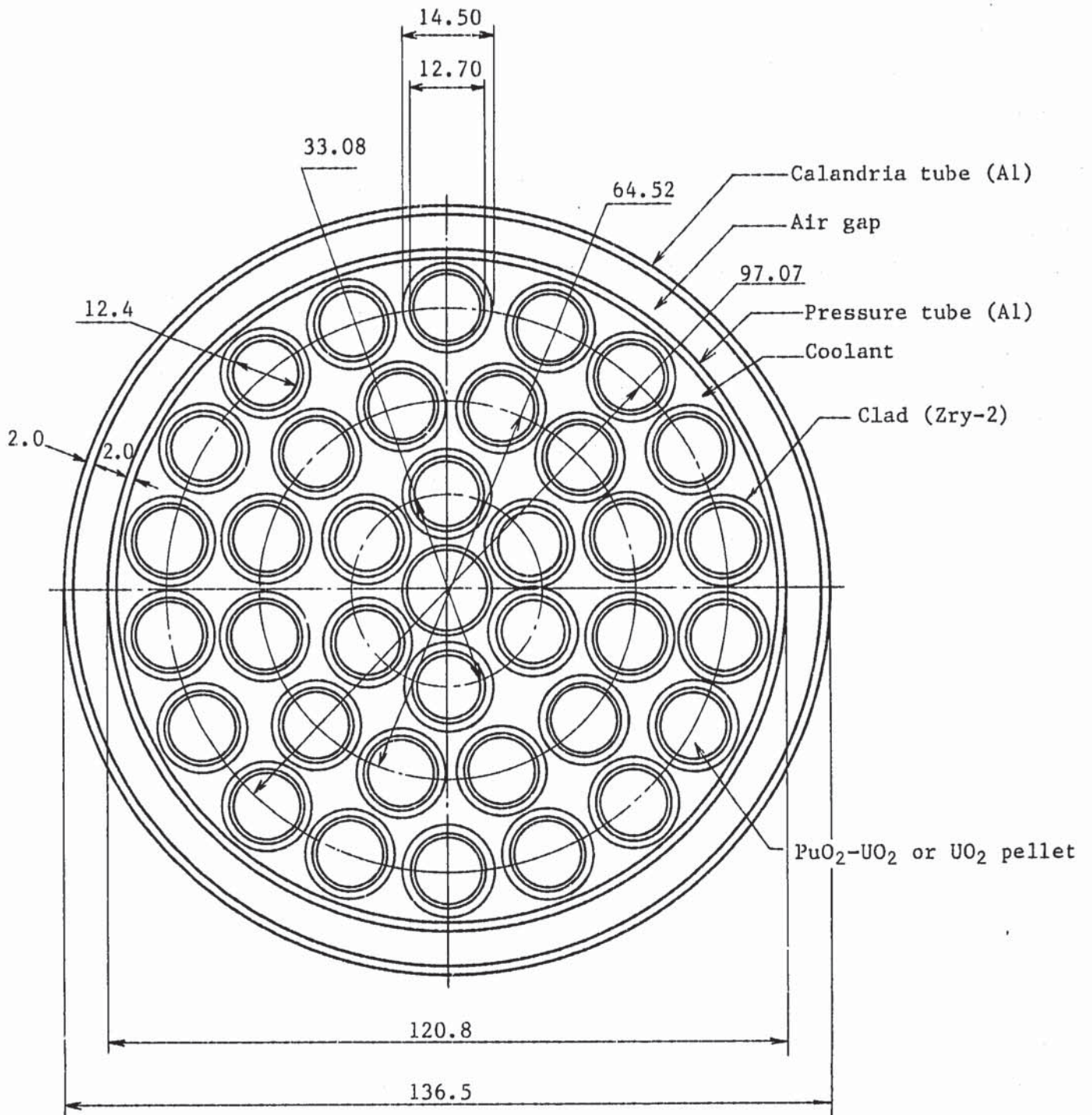


Fig. 1.2 Cross-sectional view of Type I~V 36-rod test cluster.

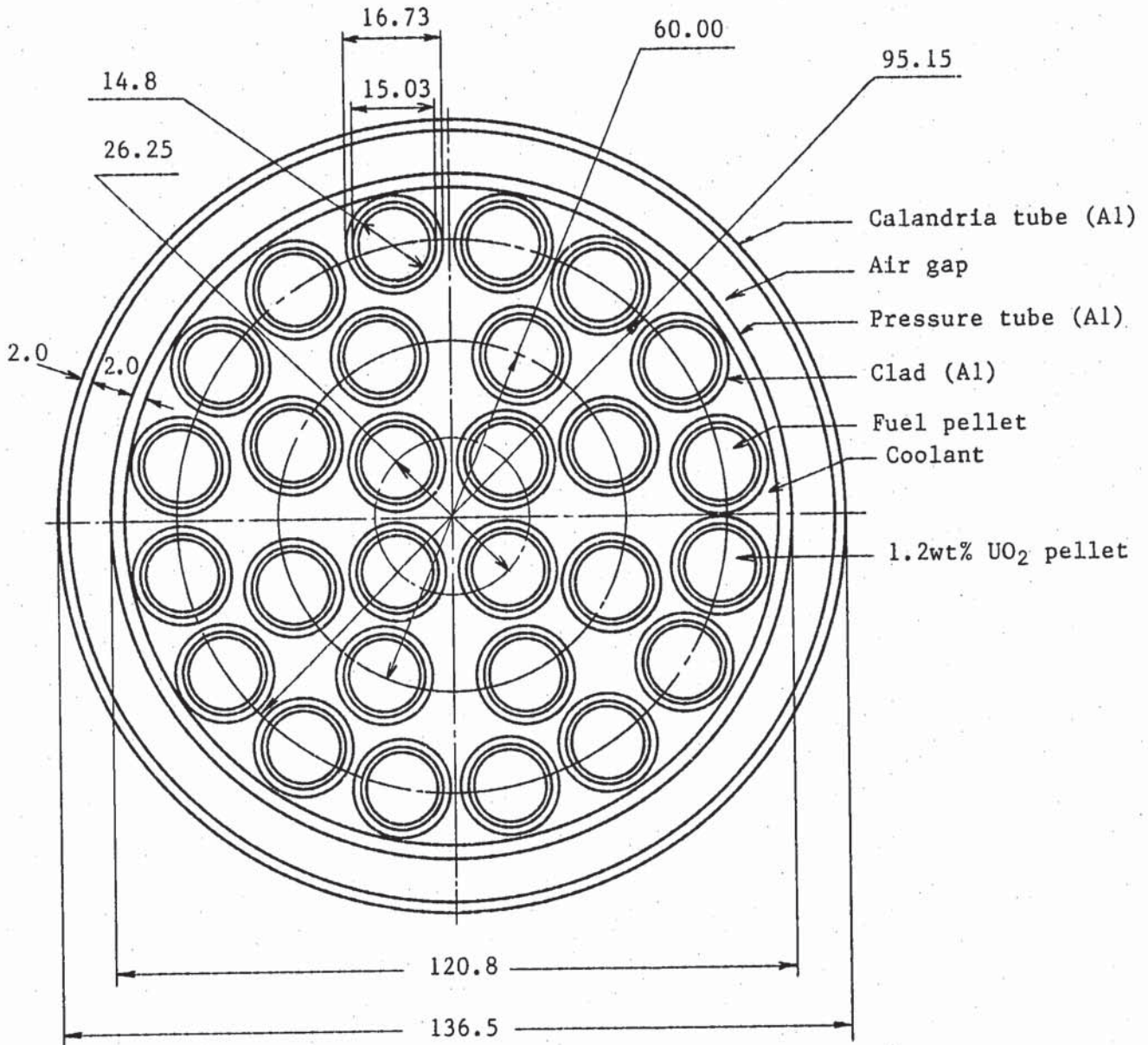


Fig. 1.3 Cross-sectional view of 28-rod UO₂ cluster used in the driver region.

2. Measurement of Coolant Void Reactivity

Table 2.1 Level Reactivity Coefficient of Moderator and Critical Level of the Core Fueled with 36-rod UO₂ Test Clusters.

Table 2.2 Level Reactivity Coefficient of Moderator and Critical Level of the Core Fueled with 36-rod MOX Test Clusters.

Table 2.3 Result of Fitting Parameters by Least-Squares Method for Critical Level vs. Level Reactivity Coefficient of Moderator.

Table 2.4 Experimental Void Reactivity in the Core Fueled with 36-rod UO₂ Test Clusters.

Table 2.5 Experimental Void Reactivity in the Core Fueled with 36-rod MOX Test Cluster.

Fig. 2.1 Relation between level reactivity coefficient of moderator and critical level of the core fueled with 36-rod UO₂ test clusters.

Fig. 2.2 Relation between level reactivity coefficient of moderator and critical level of the core fueled with 36-rod MOX test cluster.

Fig. 2.3 Coolant void reactivity due to change in void fraction from 0%.

Table 2.1 Level Reactivity Coefficient of Moderator
and Critical Level of the Core Fueled with
36-rod UO₂ Test Clusters

Fuel Type		Void Fraction (%)		Position of B ₄ C Rods Inserted	Coolant Level (mm)	Critical Level H(mm)	$\Delta\rho/\Delta H$ (d/cm)	Temperature (°C)
Test Ch. (Center)	Central 8Ch.	Center	8ch.					
I	I	0	0	-	1240	1230.2	16.3±0.3	25.5
				-	1230	1230.1	15.7±0.3	25.5
		30	30	-	1310	1303.6	15.4±0.3	25.0
				-	1310	1303.0	15.7±0.3	25.0
		70	70	-	1410	1413.0	13.7±0.2	25.0
				-	1410	1412.8	13.8±0.2	25.0
		100	100	-	0	1458.6	15.1±0.3	24.5
-	0			1458.6	15.6±0.3	24.5		
0	100	-	1400	1402.8	15.4±0.3	25.0		
		-	1400	1402.9	15.4±0.3	25.0		
		30	100	-	1420	1422.5	15.8±0.3	24.5
				-	1420	1422.8	14.9±0.2	24.5
		70	100	-	1480	1448.8	14.6±0.4	24.5
-	1450			1448.8	14.6±0.4	24.5		
II	I	0	0	-	1230	1248.3	15.6±0.2	25.2
				-	1247	1247.0	15.3±0.2	25.2
				-	1247	1245.5	16.2±0.3	28.5
		100	100	-	0	1466.0	14.4±0.2	24.0
				-	0	1465.4	15.1±0.3	24.0
0	100	-	1410	1419.0	15.3±0.2	25.0		
		-	1420	1418.8	15.0±0.2	25.0		
I	I	30	30	3A5	1330	1337.2	14.3±0.2	25.0
					1337	1336.4	13.9±0.2	25.0
		70	70	3A5, 5C5	1390	1357.1	13.7±0.3	25.0
					1360	1356.8	13.5±0.3	25.0
				3A5	1450	1459.5	12.6±0.2	24.5
					1459	1459.3	12.8±0.2	24.5
		3A5, 5C5		1480	1489.6	11.7±0.3	24.0	
1489	1488.9			11.7±0.3	24.0			
100	100	5A1	0	1530.5	12.9±0.2	24.0		
			0	1530.6	13.0±0.2	24.0		
5C5, 7A3		0	1506.6	13.7±0.3	24.0			
		0	1506.1	13.9±0.3	24.0			

Table 2.2 Level Reactivity Coefficient of Moderator
and Critical Level of the Core Fueled with
36-rod MOX Test Cluster

Fuel Type		Void Fraction (%)		Position of B ₄ C Rods Inserted	Coolant Level (mm)	Critical Level H(mm)	$\Delta\rho/\Delta H$ (ϕ/cm)	Temperature ($^{\circ}C$)
Test Ch. (Center)	Central 8Ch.	Center	8ch.					
III	I	0	0	-	1200	1209.4	16.8±0.3	27.5
				-	1200	1209.4	17.6±0.4	27.5
		0	100	-	1399	1398.3	15.9±0.3	27.5
				-	1420	1422.8	14.9±0.3	27.5
		30	100	-	1420	1422.6	15.5±0.3	27.5
				-	1430	1443.0	14.5±0.3	27.5
		70	100	-	1443	1443.0	14.3±0.3	27.5
				-	0	1439.6	14.9±0.3	27.0
		100	100	-	0	1439.5	15.0±0.3	27.0
				-				
IV	I	0	0	-	1260	1254.5	16.5±0.3	29.0
				-	1260	1254.4	16.9±0.3	29.0
		0	100	-	1440	1440.6	15.3±0.3	29.0
				-	0	1471.2	14.9±0.3	28.5
V	I	0	0	-	1280	1272.8	15.8±0.3	29.0
				-	1280	1272.9	15.8±0.3	29.0
		30	30	-	1350	1350.3	14.3±0.2	28.5
				-	1350	1349.5	14.3±0.2	28.5
		70	70	-	1445	1450.6	13.1±0.2	29.5
				-	1451	1450.2	13.2±0.2	29.5
		100	100	-	0	1481.6	14.4±0.2	29.0
				-				
		0	100	-	1458	1458.0	14.6±0.3	29.0
				-	1458	1457.8	14.7±0.3	29.0
		30	100	-	1460	1476.2	14.2±0.2	29.0
				-	1475	1475.8	14.1±0.2	29.0
		70	100	-	1482	1491.3	14.3±0.2	29.0
				-	1490	1490.8	14.2±0.2	29.0
30	30	3A5	1400	1387.9	13.6±0.2	29.5		
		3A5, 5C5	1390	1387.8	13.6±0.2	29.5		
70	70	5C5	1400	1414.0	12.7±0.2	29.0		
		5C5, 3A5	1415	1412.6	12.7±0.2	29.0		
70	70	5C5	1490	1476.4	12.5±0.2	29.5		
		5C5, 3A5	1477	1476.4	12.5±0.2	29.5		
1520	1535	5C5, 3A5	1520	1535.2	11.0±0.2	29.5		
		5C5, 3A5	1535	1534.2	11.1±0.2	29.5		
1534.5	1570.3	3A5	0	1534.5	13.5±0.3	28.5		
		3A5, 5C5	0	1570.3	12.9±0.3	28.0		

Table 2.3 Result of Fitting Parameters by Least-Squares Method for Critical Level vs. Level Reactivity Coefficient of Moderator

Fuel Type		Void Fraction in Central 9Ch. (%)	C* ($\times 10^5$ cm ²)	λ^* (cm)
Test Ch. (Center)	Central 8Ch.			
I or II	I	0	2.050 \pm 0.010	-14.61
		30	1.876 \pm 0.010	-23.95
		70	2.993 \pm 0.011	-12.10
		100	4.066 \pm 0.014	-7.08
III, IV or V	I	0	1.702 \pm 0.017	-23.67
		30	1.938 \pm 0.013	-23.97
		70	2.675 \pm 0.020	-18.10
		100	3.858 \pm 0.018	-9.46

$$* (\Delta\rho/\Delta H) = C(H + \lambda)^{-3}$$

Table 2.4 Experimental Void Reactivity in the Core Fueled with 36-rod UO₂ Test Clusters

(1) Constant Axial Buckling due to Voiding

Fuel Type		Change in Void Fraction		Axial Buckling before Voiding	Void Reactivity		
Test Ch. (Center)	Central 8Ch.*	No. of Voiding Ch.	Extent of Voiding (%)	(m ⁻²)	$\rho_{v \rightarrow v'}$ (§)		
I	I	9 (3×3)	0 → 30	5.22 ± 0.05	-1.30 ± 0.12		
			0 → 70	5.22 ± 0.05	-3.31 ± 0.13		
			0 → 100	5.22 ± 0.05	-4.94 ± 0.15		
			30 → 70	4.69 ± 0.05	-1.80 ± 0.11		
			30 → 100	4.69 ± 0.05	-3.09 ± 0.13		
			70 → 100	4.04 ± 0.04	-0.88 ± 0.11		
		1 (Center)	0 → 30	4.05 ± 0.04	-0.30 ± 0.11		
			0 → 70	4.05 ± 0.04	-0.71 ± 0.11		
			0 → 100	4.05 ± 0.04	-0.90 ± 0.12		
			30 → 70	3.95 ± 0.03	-0.40 ± 0.11		
			30 → 100	3.95 ± 0.03	-0.57 ± 0.11		
			70 → 100	3.82 ± 0.03	-0.15 ± 0.11		
		8 (3×3 except center)	0 → 100	5.22 ± 0.05	-3.67 ± 0.14		
			30 → 100	4.69 ± 0.05	-2.30 ± 0.12		
			70 → 100	4.04 ± 0.04	-0.70 ± 0.11		
		II	I	9	0 → 100	5.09 ± 0.05	-4.59 ± 0.15
				1	0 → 100	3.96 ± 0.04	-0.74 ± 0.11
				8	0 → 100	5.09 ± 0.05	-3.51 ± 0.14

* (3×3) channels except center

(2) Constant Core Height due to Voiding

Fuel Type		Change in Void Fraction		Critical Level of unchanged Core (cm)	Void Reactivity $\rho_{v \rightarrow v'}$ (β)
Test Ch. (Center)	Central 8Ch.*	No. of Voiding Ch.	Extent of Voiding (%)		
I	I	9 (3x3)	0 → 30	123.01	-1.26 ± 0.12
			0 → 70	123.01	-3.20 ± 0.13
			0 → 100	123.01	-4.57 ± 0.15
			30 → 70	130.30	-1.74 ± 0.11
			30 → 100	130.30	-2.83 ± 0.13
			70 → 100	141.28	-0.73 ± 0.11
		1 (Center)	0 → 30	140.28	-0.30 ± 0.11
			0 → 70	140.28	-0.71 ± 0.11
			0 → 100	140.28	-0.90 ± 0.11
			30 → 70	142.25	-0.39 ± 0.11
			30 → 100	142.25	-0.57 ± 0.11
			70 → 100	144.88	-0.15 ± 0.11
		8 (3x3 except center)	0 → 100	123.01	-3.31 ± 0.14
			30 → 100	130.30	-2.04 ± 0.12
			70 → 100	141.28	-0.55 ± 0.11
II	I	9	0 → 100	124.70	-4.24 ± 0.15
		1	0 → 100	141.88	-0.73 ± 0.11
		8	0 → 100	124.70	-3.16 ± 0.14

* (3x3) channels except center

Table 2.5 Experimental Void Reactivity in the Core Fueled with 36-rod MOX Test Cluster

(1) Constant Axial Buckling due to Voiding

Fuel Type		Change in Void Fraction		Axial Buckling before Voiding (m^{-2})	Void Reactivity $\rho_{V \rightarrow V^-}$ ($\$$)
Test Ch. (Center)	Central 8Ch.*	No. of Voiding Ch.	Extent of Voiding (%)		
V	I	9 (3×3)	0 → 30	4.91 ± 0.05	-1.25 ± 0.07
			0 → 70	4.91 ± 0.05	-3.02 ± 0.08
			0 → 100	4.91 ± 0.05	-4.20 ± 0.09
			30 → 70	4.41 ± 0.04	-1.54 ± 0.07
			30 → 100	4.41 ± 0.04	-2.46 ± 0.07
			70 → 100	3.85 ± 0.03	-0.61 ± 0.06
IV	I	9(3×3)	0 → 100	5.04 ± 0.05	-4.51 ± 0.09
III	I	9(3×3)	0 → 100	5.38 ± 0.06	-5.19 ± 0.10
V	I	1 (Center)	0 → 30	3.78 ± 0.03	-0.26 ± 0.06
			0 → 70	3.78 ± 0.03	-0.48 ± 0.06
			0 → 100	3.78 ± 0.03	-0.35 ± 0.06
			30 → 70	3.69 ± 0.03	-0.22 ± 0.06
			30 → 100	3.69 ± 0.03	-0.08 ± 0.06
			70 → 100	3.63 ± 0.03	0.13 ± 0.06
IV	I	1(Center)	0 → 100	3.86 ± 0.03	-0.47 ± 0.07
III	I	1 (Center)	0 → 30	4.07 ± 0.04	-0.38 ± 0.07
			0 → 70	4.07 ± 0.04	-0.68 ± 0.07
			0 → 100	4.07 ± 0.04	-0.66 ± 0.07
			30 → 70	3.95 ± 0.03	-0.30 ± 0.06
			30 → 100	3.95 ± 0.03	-0.26 ± 0.07
			70 → 100	3.85 ± 0.03	0.05 ± 0.06

* (3×3) channels except center

(2) Constant Core Height due to Voiding

Fuel Type		Change in Void Fraction		Critical Level of unchanged Core (cm)	Void Reactivity $\rho_{v \rightarrow v'}$ ($\$$)
Test Ch. (Center)	Central 8Ch.*	No. of Voiding Ch.	Extent of Voiding (%)		
V	I	9 (3x3)	0 → 30	127.28	-1.21 ± 0.07
			0 → 70	127.28	-2.92 ± 0.08
			0 → 100	127.28	-3.87 ± 0.09
			30 → 70	134.95	-1.49 ± 0.07
			30 → 100	134.95	-2.22 ± 0.07
			70 → 100	145.02	-0.47 ± 0.06
IV	I	9(3x3)	0 → 100	125.44	-4.16 ± 0.09
III	I	9(3x3)	0 → 100	120.94	-4.79 ± 0.10
V	I	1 (Center)	0 → 30	145.78	-0.26 ± 0.06
			0 → 70	145.78	-0.48 ± 0.06
			0 → 100	145.78	-0.35 ± 0.06
			30 → 70	147.58	-0.22 ± 0.06
			30 → 100	147.58	-0.08 ± 0.06
			70 → 100	149.08	0.13 ± 0.06
IV	I	1 (Center)	0 → 100	144.06	-0.47 ± 0.07
III	I	1 (Center)	0 → 30	139.83	-0.38 ± 0.07
			0 → 70	139.83	-0.68 ± 0.07
			0 → 100	139.83	-0.66 ± 0.07
			30 → 70	142.26	-0.30 ± 0.06
			30 → 100	142.26	-0.26 ± 0.07
			70 → 100	144.30	0.05 ± 0.06

* (3x3) channels except center

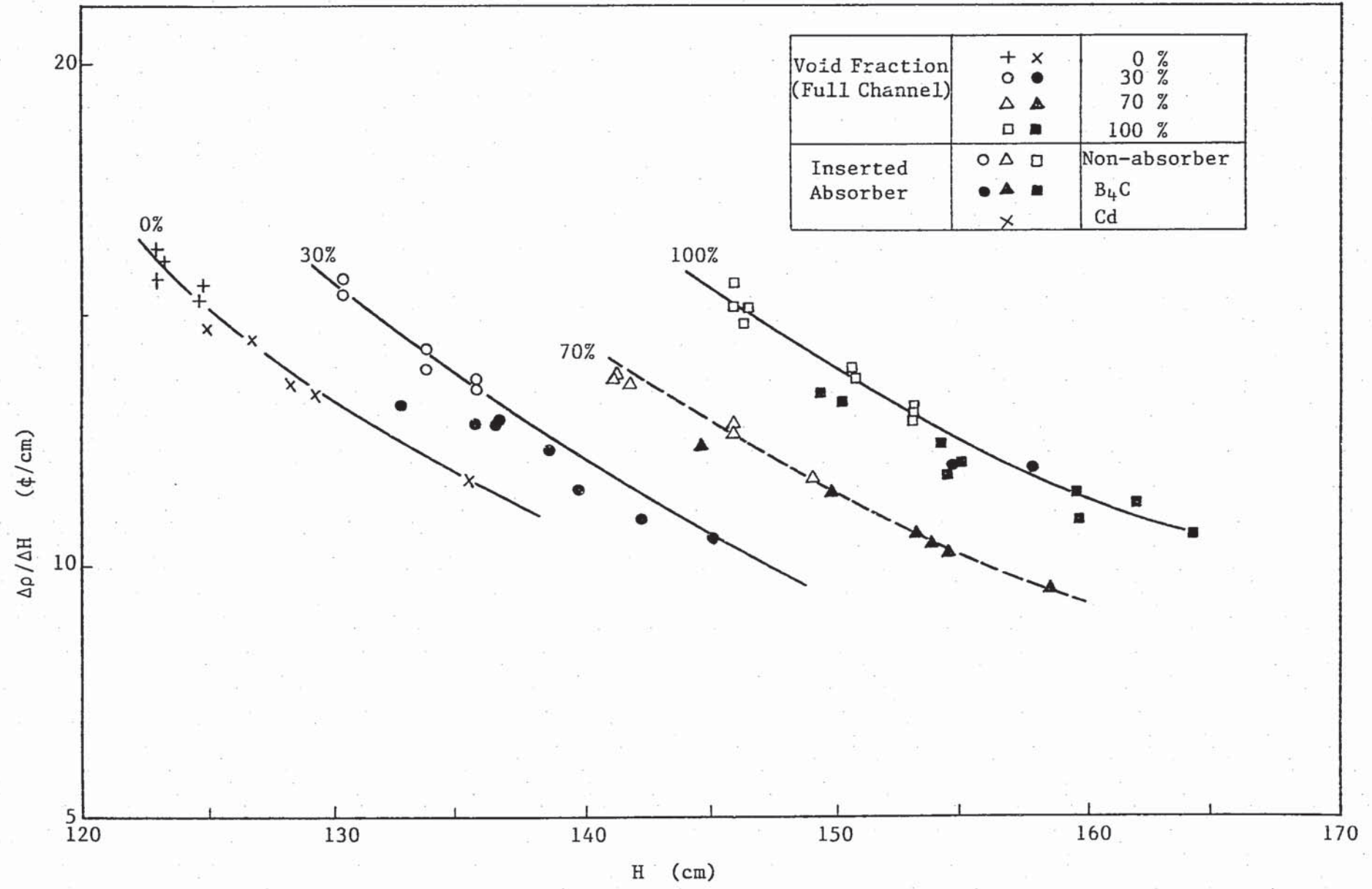


Fig. 2.1 Relation between level reactivity coefficient of moderator and critical level of the core fueled with 36-rod UO_2 test clusters.

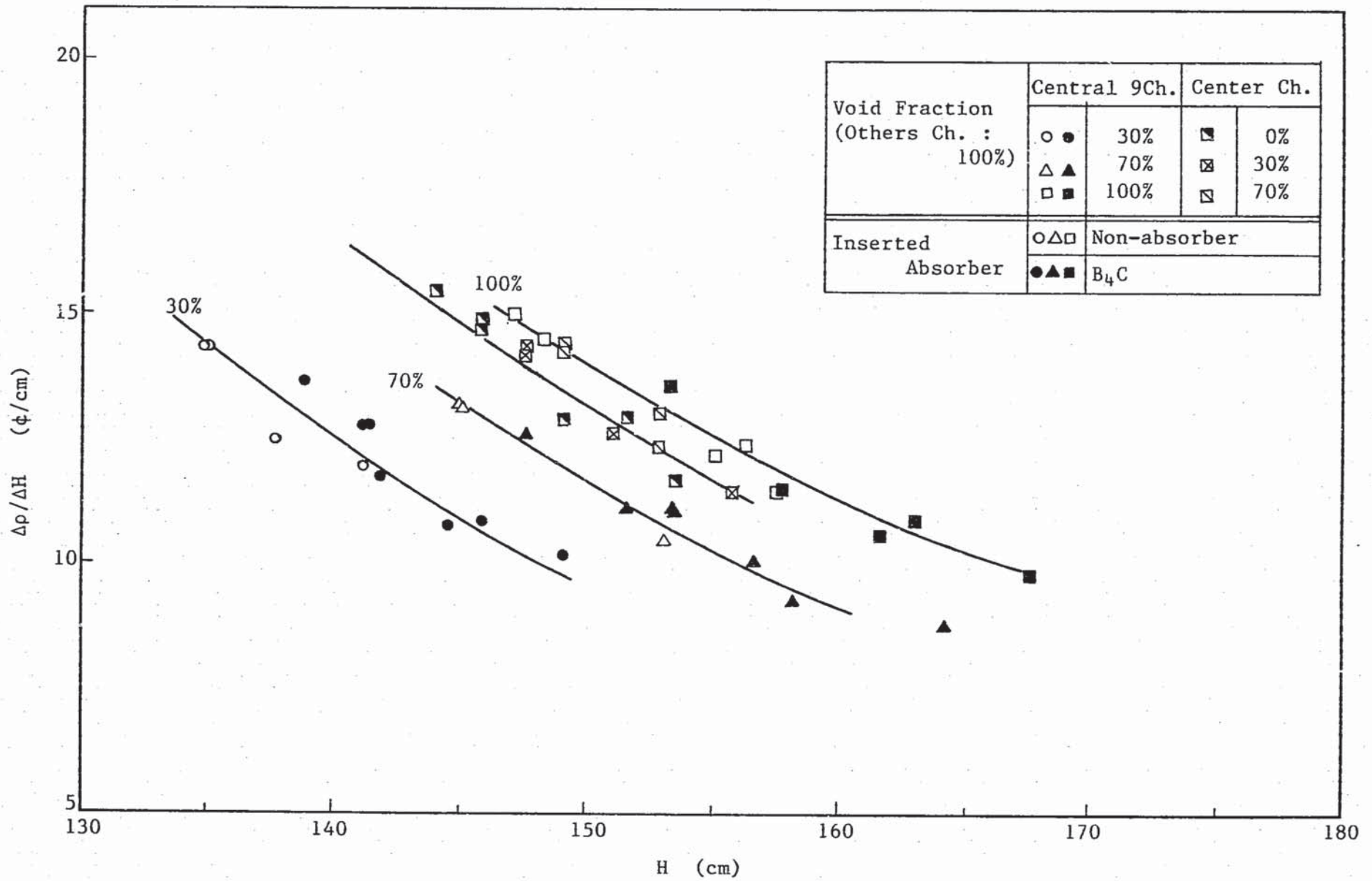


Fig. 2.2 Relation between level reactivity coefficient of moderator and critical level of the core fueled with 36-rod MOX test cluster.

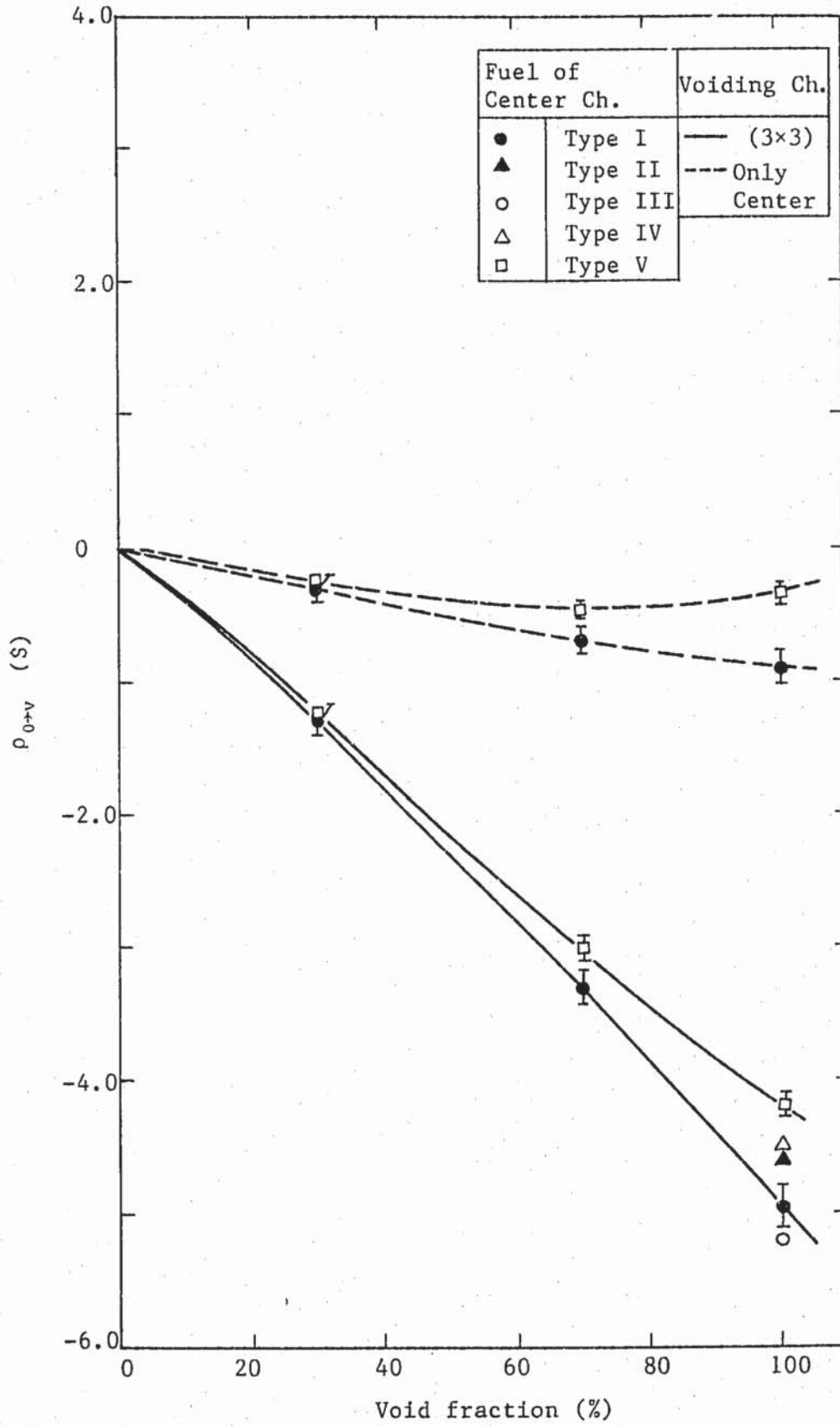


Fig Fig. 2.3 Coolant void reactivity due to change in void fraction from 0%.

3. Measurement of Axial Reflection Saving

Table 3.1 Extrapolation Length by Copper Activation Method

- Fig. 3.1 Dependence of axial buckling on fitting range in the non-voided region of core.
- Fig. 3.2 Dependence of axial buckling on fitting range in the 30%-voided region of core.
- Fig. 3.3 Dependence of axial buckling on fitting range in the 70%-voided region of core.
- Fig. 3.4 Dependence of axial buckling on fitting range in the 100%-voided region of core.
- Fig. 3.5 Axial flux distribution in the non-voided region of core.
- Fig. 3.6 Axial flux distribution in the 30%-voided region of core.
- Fig. 3.7 Axial flux distribution in the 70%-voided region of core.
- Fig. 3.8 Axial flux distribution in the 100%-voided region of core.

Table 3.1 Extrapolation Length by Copper Activation Method

Void fraction in (3×3)Ch.	λ_z (cm)		Effective λ_z^{**} (cm)
	(3×3)Ch.	The Other 88Ch*	
0	13.5 ± 0.5	15.0 ± 0.5	14.5 ± 0.7
30	14.0 ± 0.5	15.0 ± 0.5	14.7 ± 0.7
70	15.0 ± 0.5	15.0 ± 0.5	15.0 ± 0.7
100	17.5 ± 0.5	15.0 ± 0.5	15.9 ± 0.7

* Void fraction is 100%.

** Volume weighted value using statistical weight 0.35.

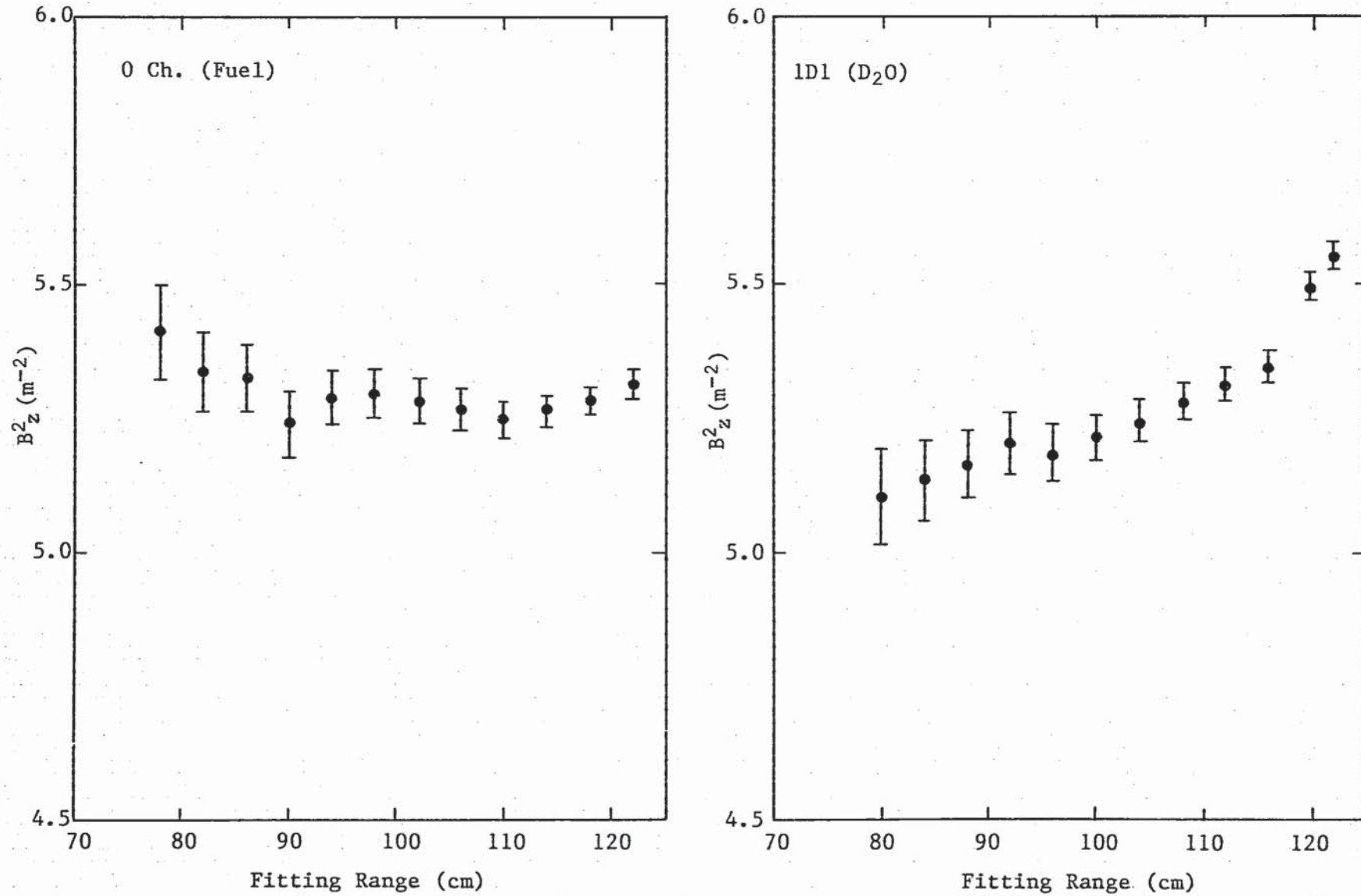


Fig. 3.1 Dependence of axial buckling on fitting range in the non-voided region of core.

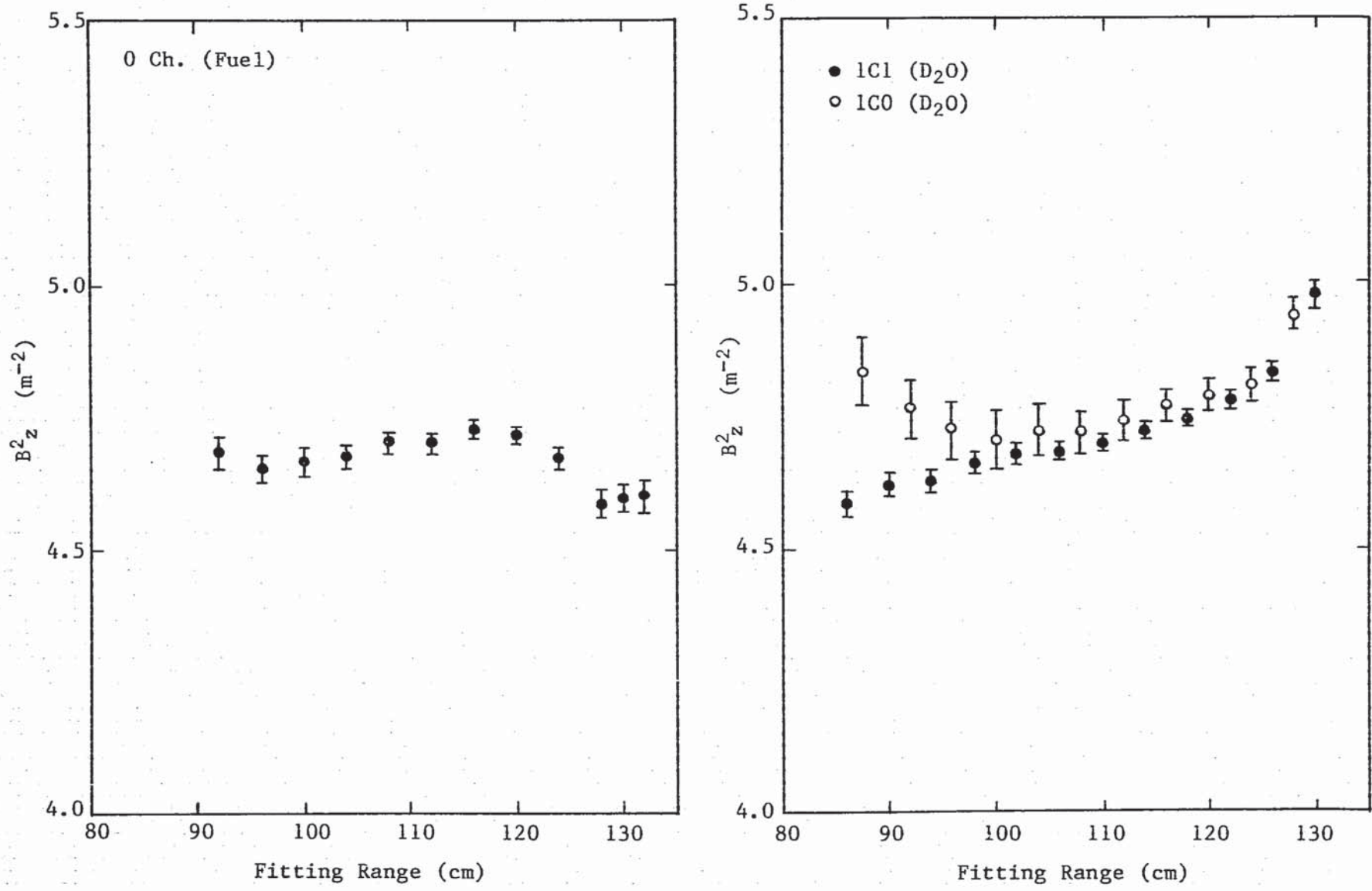


Fig. 3.2 Dependence of axial buckling on fitting range in the 30%-voided region of core.

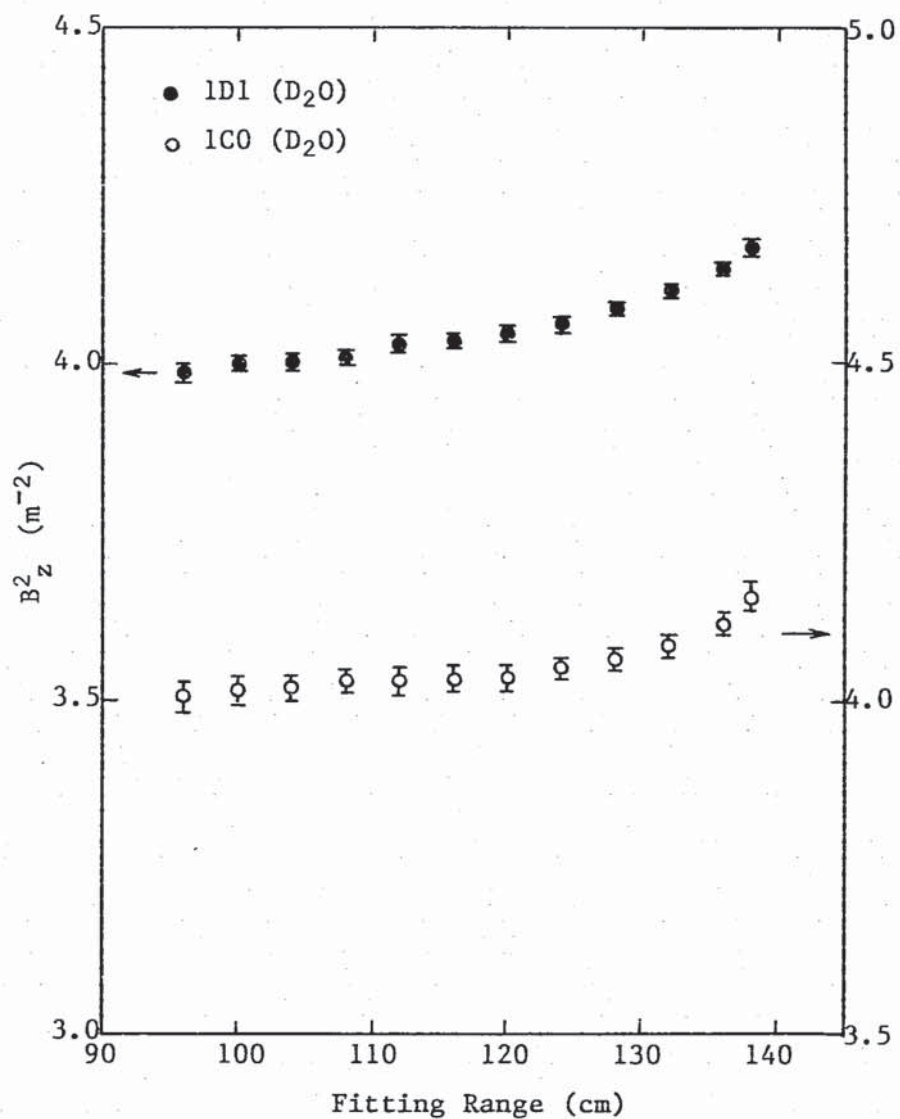
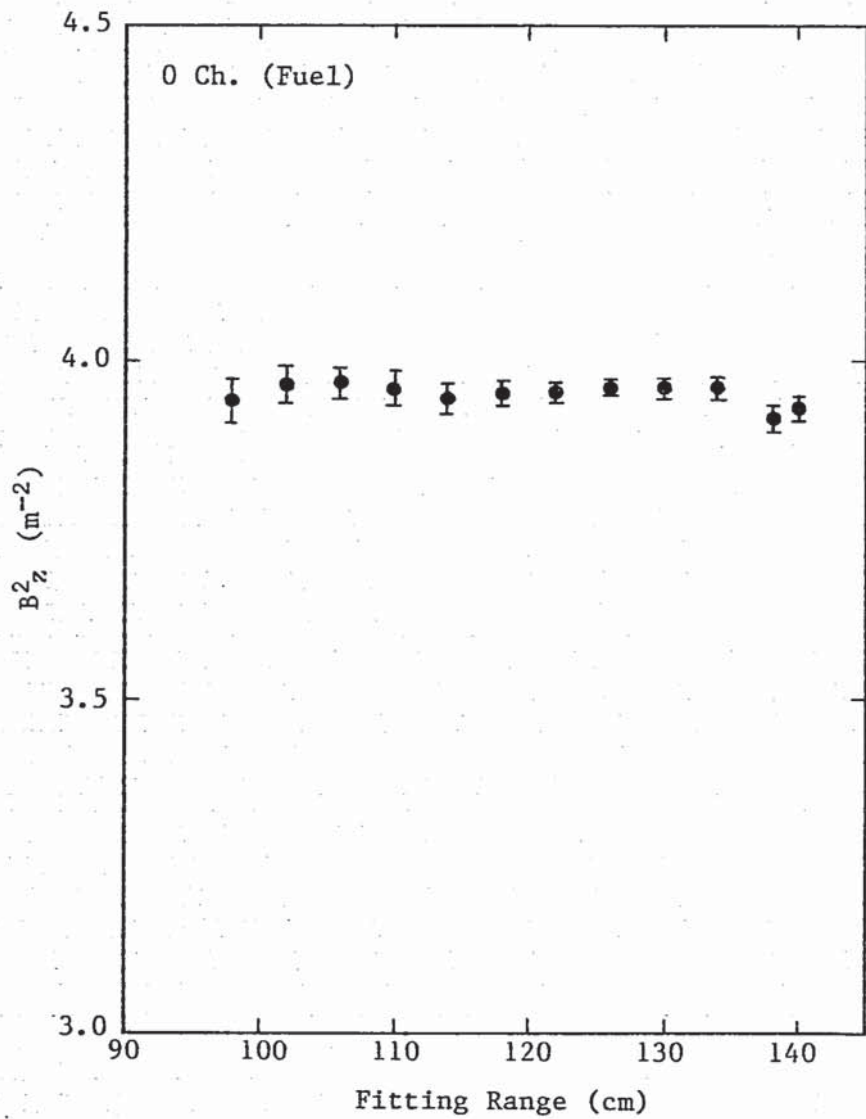


Fig. 3.3 Dependence of axial buckling on fitting range in the 70%-voided region of core.

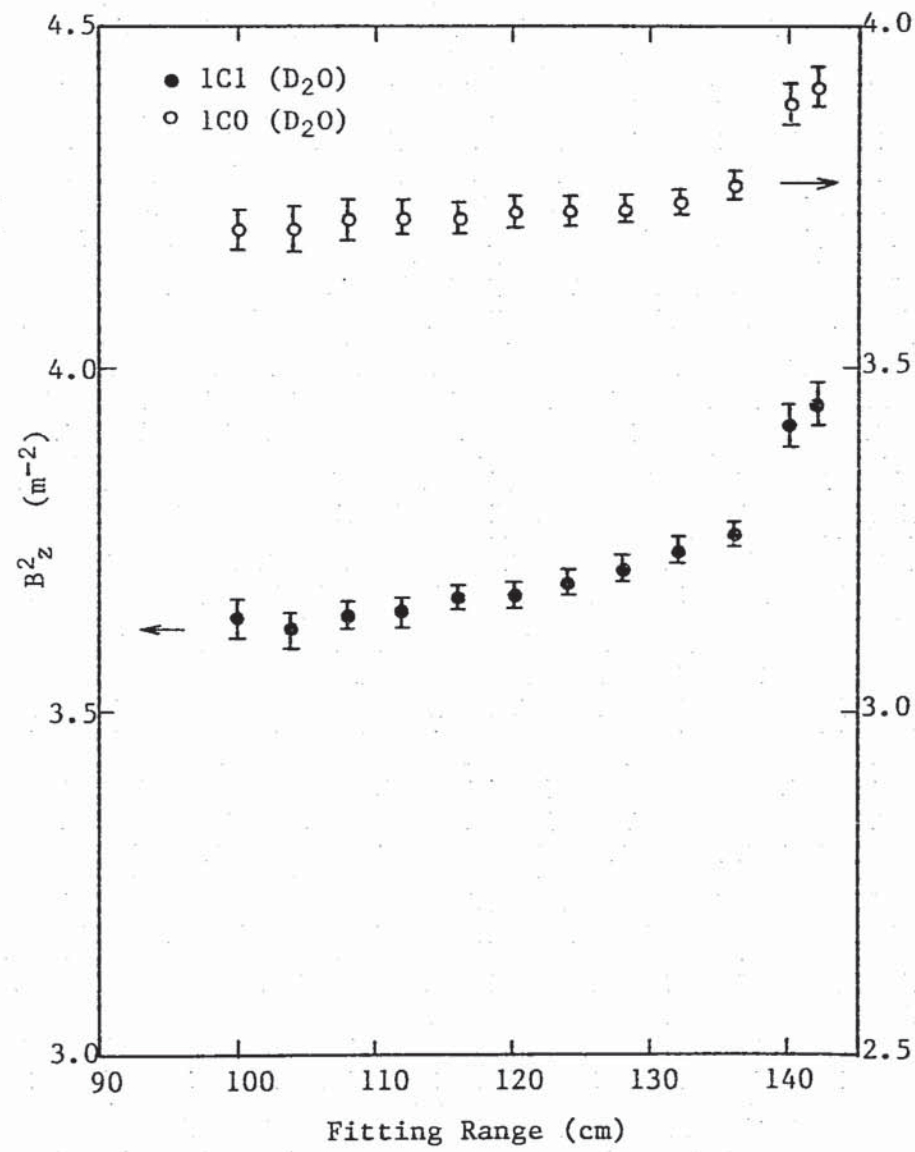
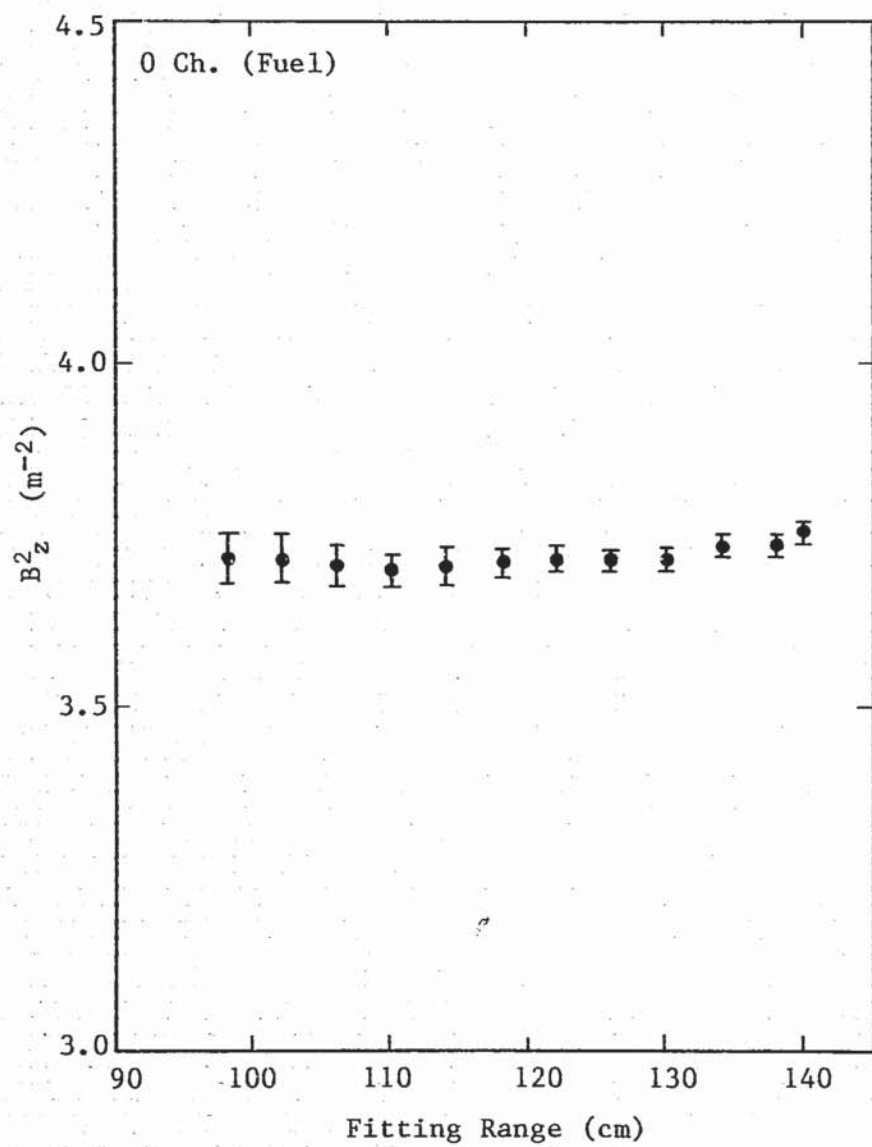
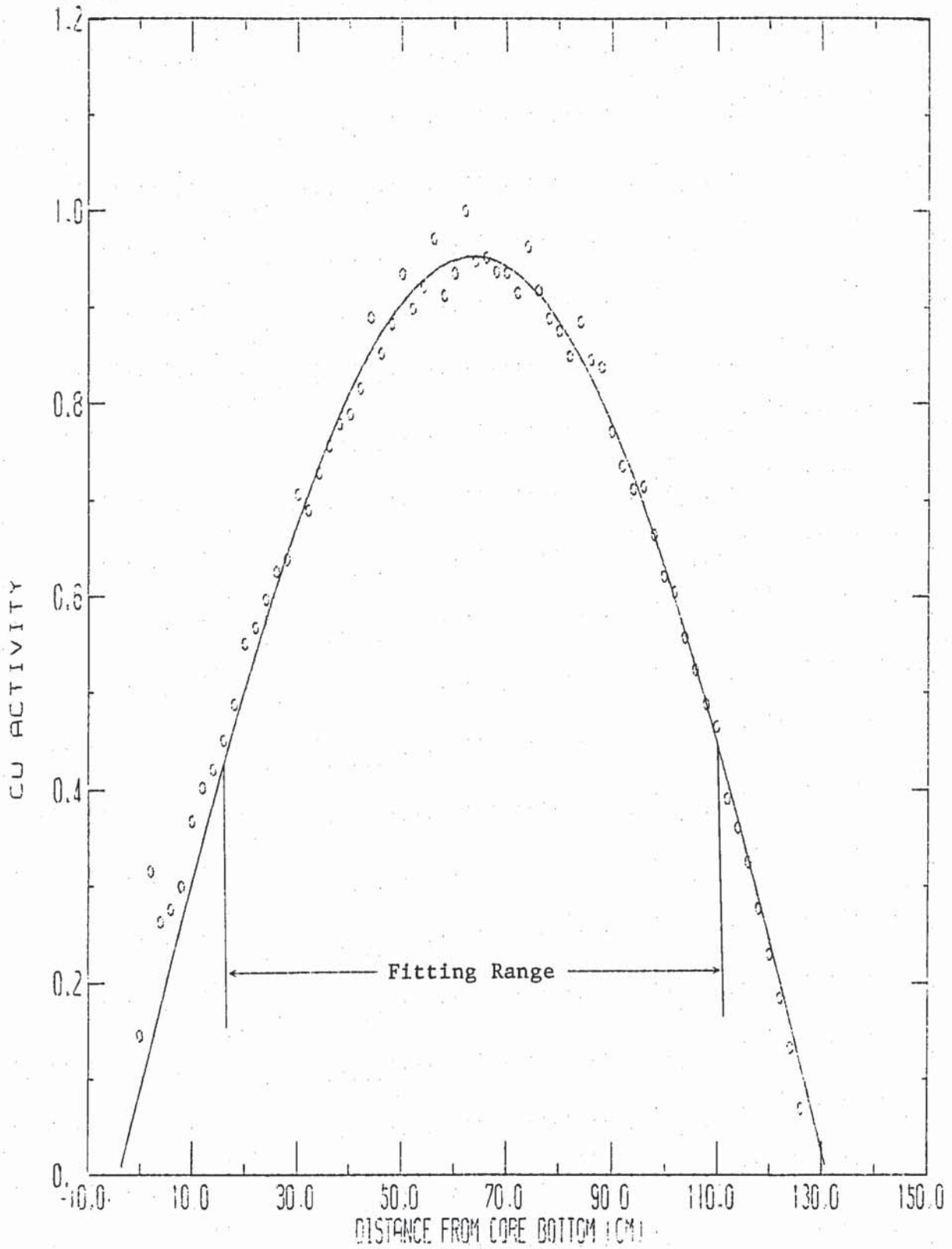
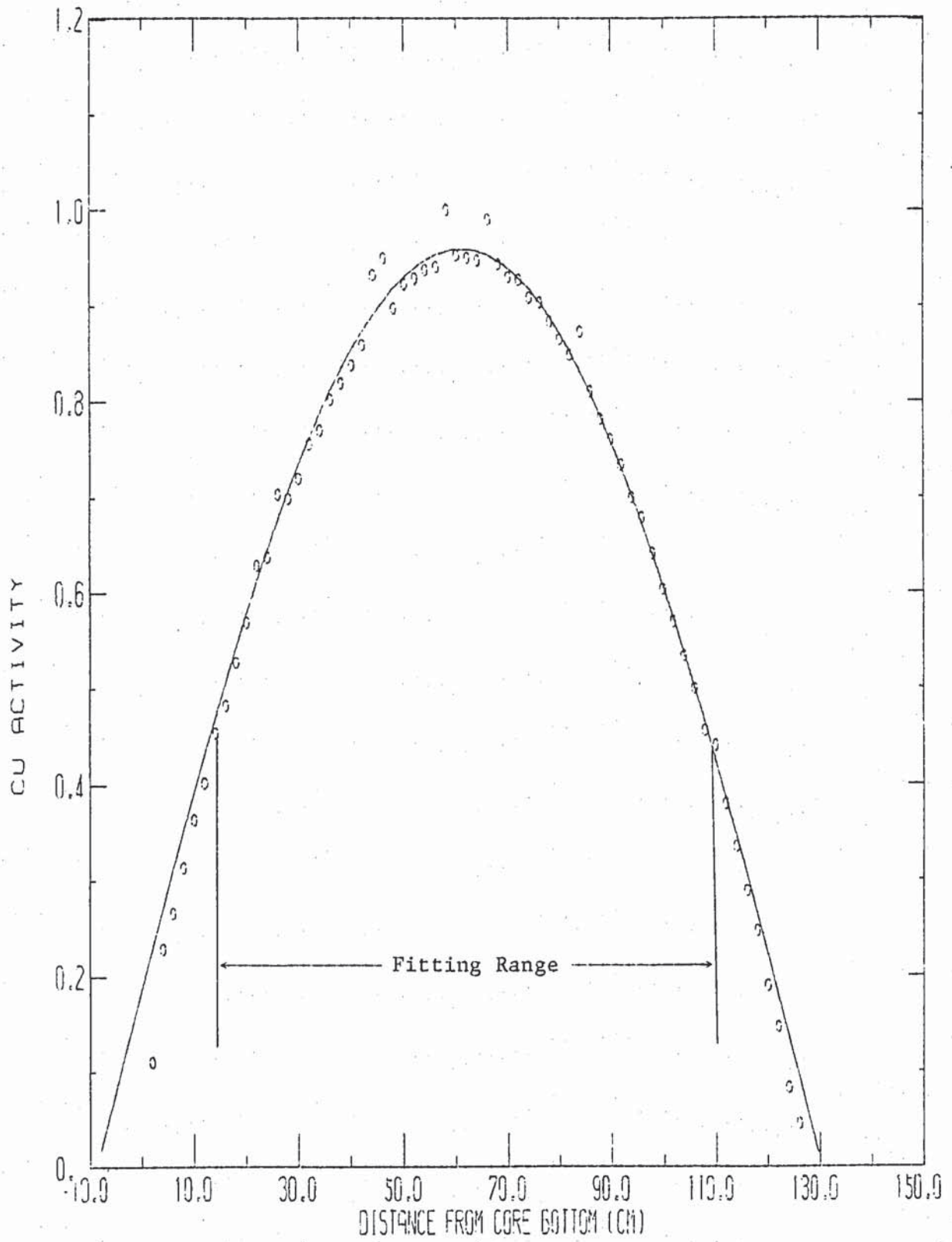


Fig. 3.4 Dependence of axial buckling on fitting range in the 100%-voided region of core.

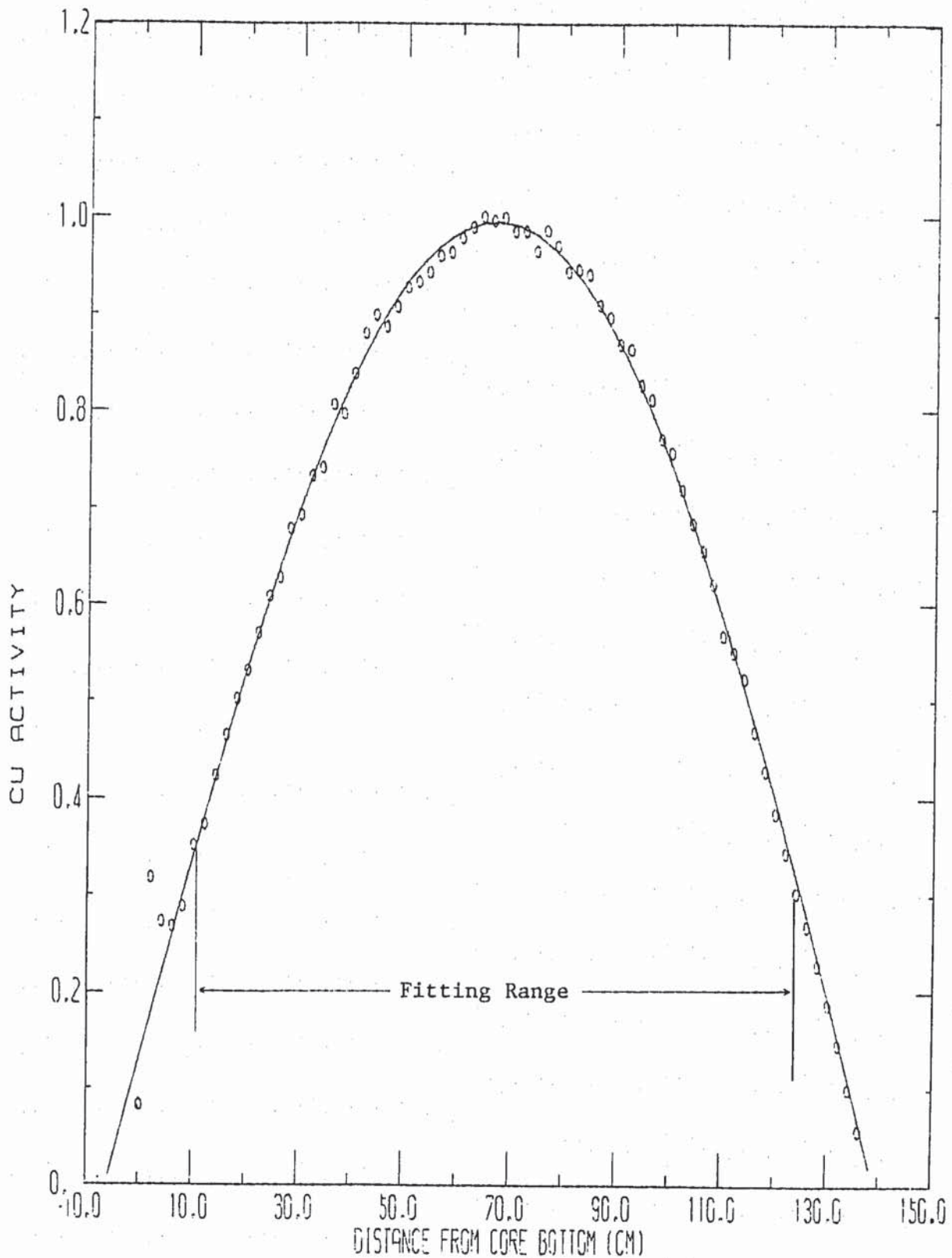


(1) Position : Fuel (0 ch)

Fig. 3.5 Axial flux distribution in the non-voided region of core.

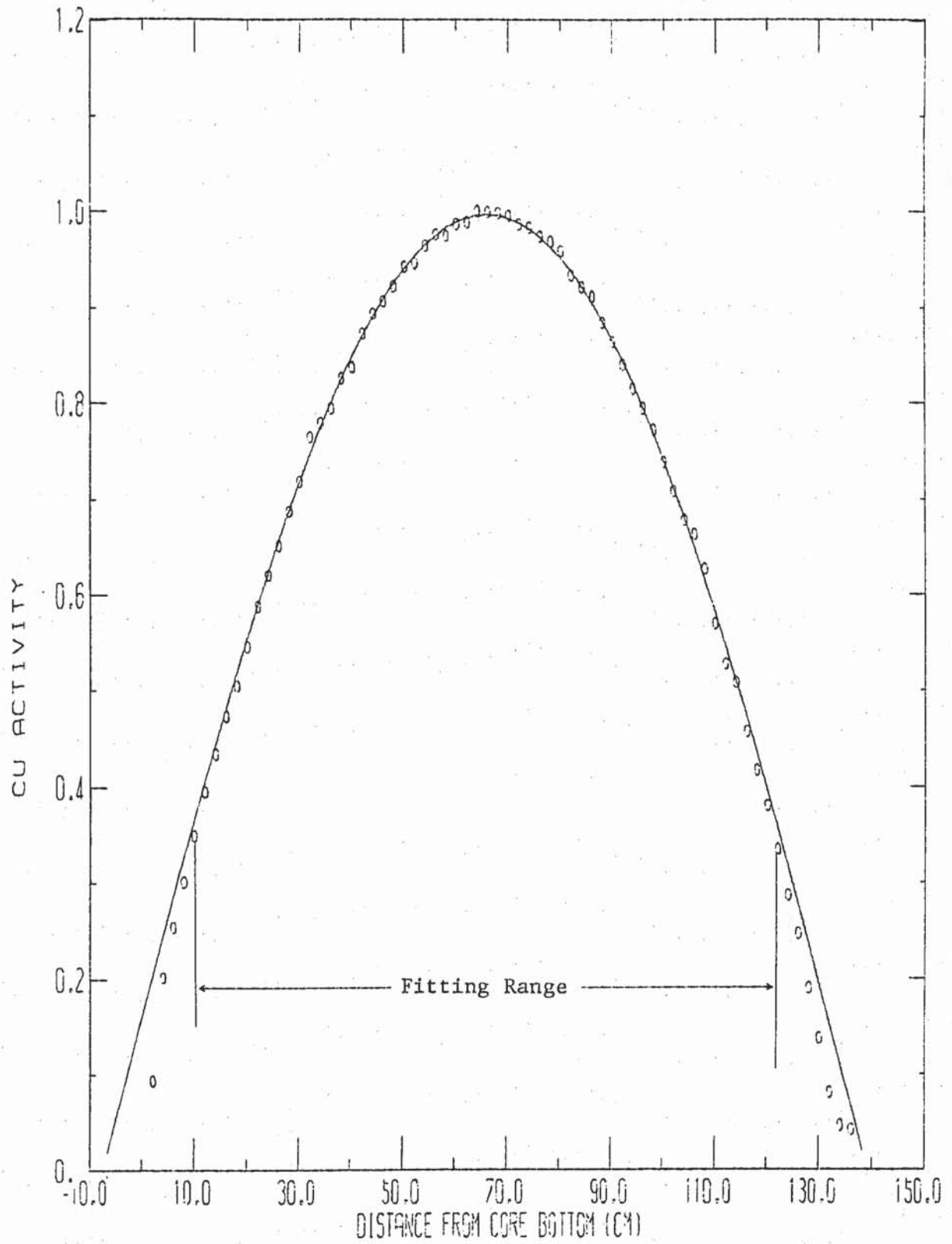


(2) Position : D₂O (1D1)

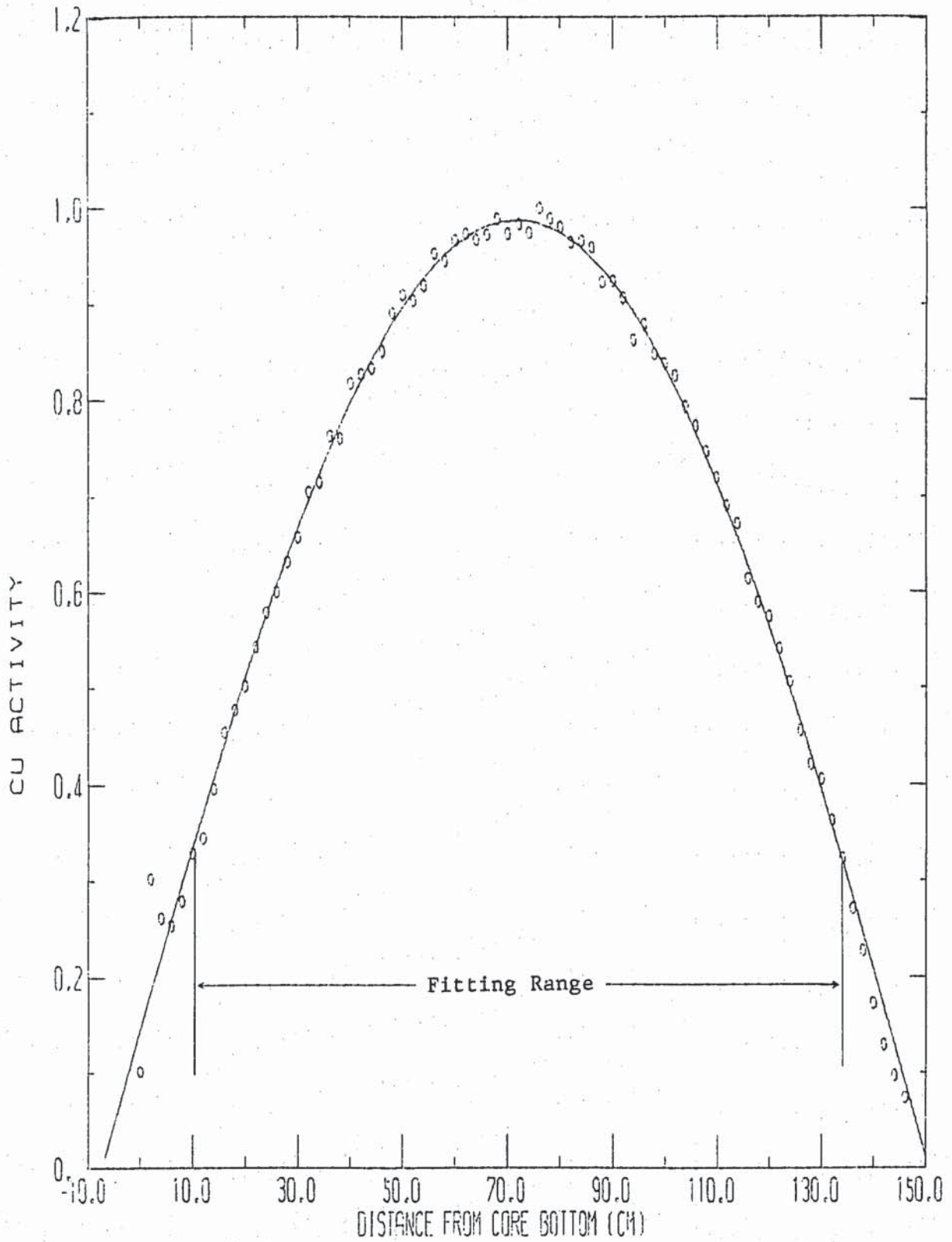


(1) Position : Fuel (0 ch)

Fig. 3.6 Axial flux distribution in the 30%-voided region of core.

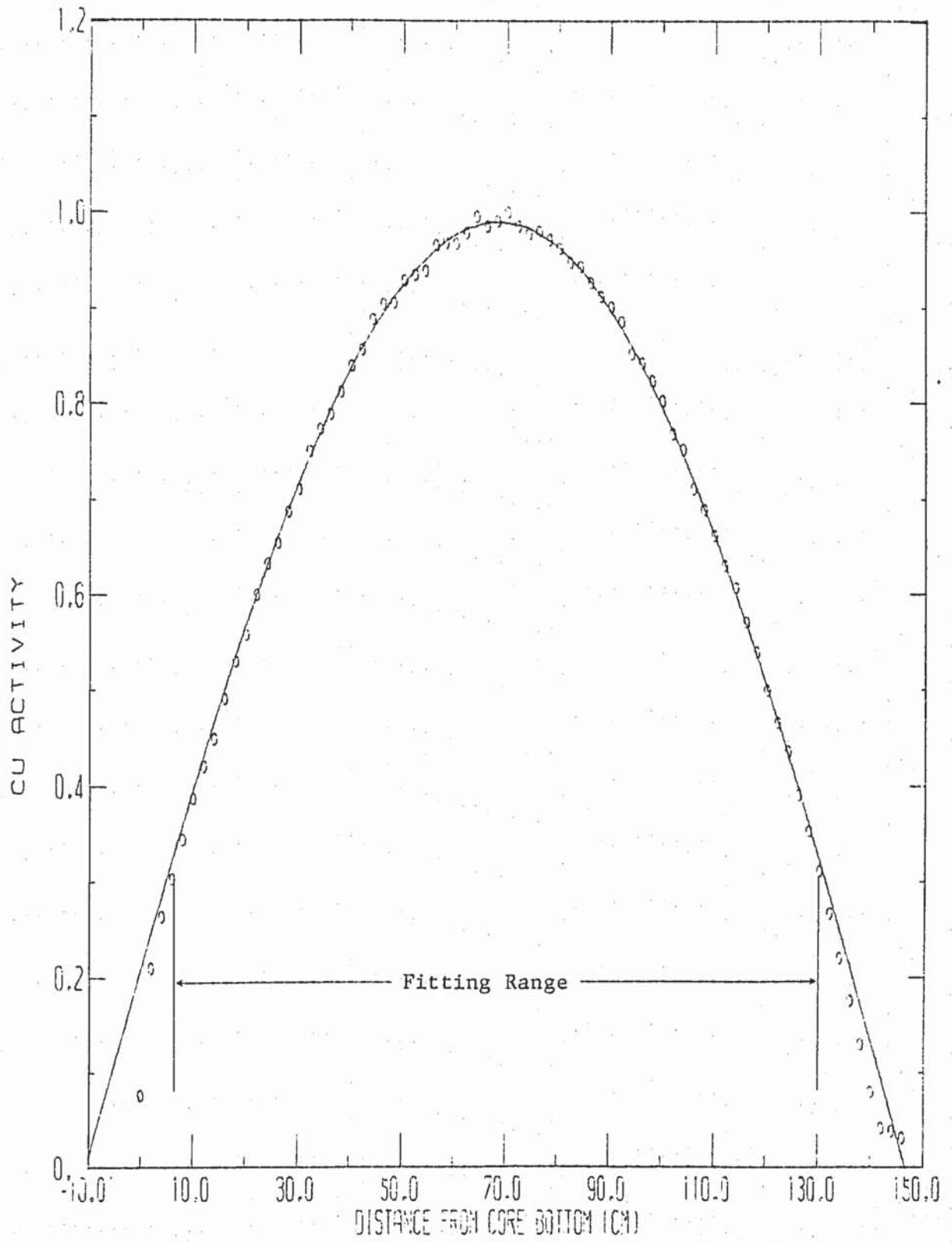


(2) Position : D₂O (1C1)

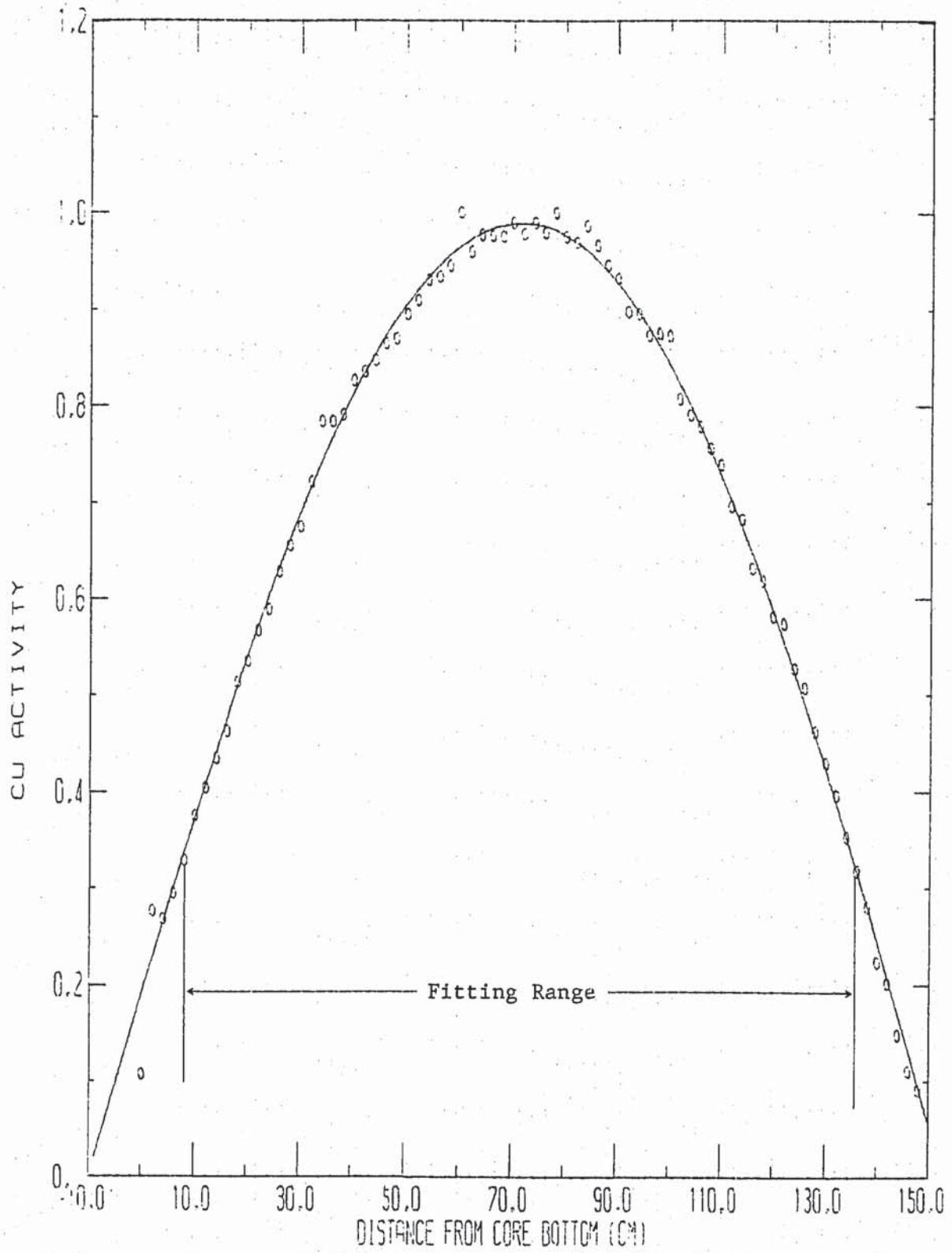


(1) Position : Fuel (0 ch)

Fig. 3.7 Axial flux distribution in the 70%-voided region of core.

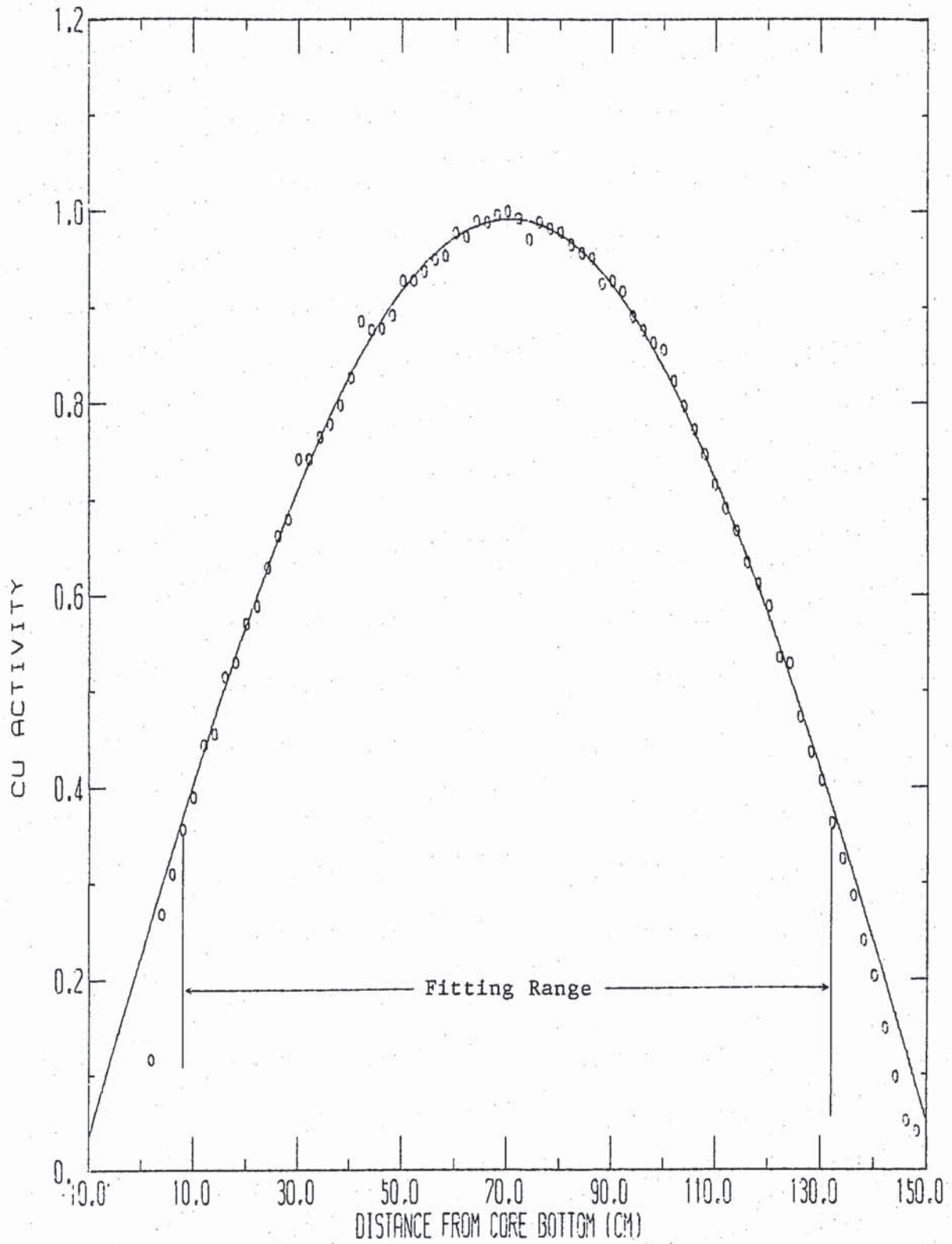


(2) Position : D₂O (1D1)



(1) Position : Fuel (0 ch)

Fig. 3.8 Axial flux distribution in the 100%-voided region of core.



(2) Position : D₂O (1C0)